Annales Societatis Geologorum Poloniae (2012), vol. 82: 239–253.

MIDDLE MIOCENE DEPOSITS IN CARPATHIAN FOREDEEP: FACIES ANALYSIS AND IMPLICATIONS FOR HYDROCARBON RESERVOIR PROSPECTING

Paweł LIS[1] & Anna WYSOCKA[2]

[1] *Polish Geological Institute, 00-975 Warsaw. Present address: Bacha St.10/701, 02-743 Warsaw, Poland, e-mail: pawel.prot.lis@gmail.com*
[2] *Faculty of Geology, University of Warsaw, al. Żwirki i Wigury 93, 02-089 Warsaw, Poland, e-mail: anna.wysocka@uw.edu.pl*

Lis, P. & Wysocka, A., 2012. Middle Miocene deposits in Carpathian Foredeep: facies analysis and implications for hydrocarbon reservoir prospecting. *Annales Societatis Geologorum Poloniae*, 82: 239–253.

Abstract: This sedimentological study was based on well cores from the Polish and Ukrainian parts of the Carpathian Foredeep. It revealed general heterogeneity of facies in the middle Miocene of the sedimentary succession in the basin. Fourteen sedimentary facies were distinguished and their origin was interpreted: massive, non-graded sandstones; normal-graded, massive sandstones, with and without a stratified uppermost part; hydroplastically deformed sandstones; planar-parallel-stratified sandstones; trough-cross-stratified sandstones; ripple-cross-laminated sandstones; heterolithic deposits, composed of thinly interlayered sandstone and mudstone; massive and laminated mudstones; and basal gypsum/anhydrite evaporites, often intercalated with mudstone. Four main modalities of vertical facies organization were recognized and attributed to the following environments: (1) the mid-late Badenian, shoal-water, evaporitic environment that preceded the latest Badenian–early Sarmatian, main phase of foredeep development; (2) a littoral, tidal environment of the inner parts of storm-influenced, coastal bays and tidal flats or possibly spit-sheltered lagoons; (3) a wave-dominated, littoral, sandy environment, considered to be shoreface, extended by waves, in front of advancing deltas; and (4) a neritic to subneritic, muddy, offshore slope, characterized by frequent incursions of tempestite and turbidite sand. The study contributed to a better understanding of the mid-Miocene depositional systems in the basin, with significant implications for ongoing hydrocarbon exploration. Interpretations of the origins of potential reservoir sandstones provided important information on their possible stratigraphic distribution in the basin fill. The potential, economic importance of stratigraphic hydrocarbon traps underscored the urgent need for a full-scale facies analysis and fully cored wells in strategic parts of the basin.

Key words: facies analysis, littoral, tidal, shoreface, neritic slope, turbidites, Markov-chain analysis.

Manuscript received 11 April 2011, accepted 20 December 2012

INTRODUCTION

The Carpathian Foredeep Basin for many decades has attracted geological interest, related to prospecting for hydrocarbon resources, with numerous geological and geophysical studies (e.g., Dziadzio *et al.*, 1997, 2006; Dziadzio, 2000; Porębski *et al.*, 2002; Kurovets *et al.*, 2004; Lyzun *et al.*, 2004; Myśliwiec *et al.*, 2004; Mastalerz *et al.*, 2006; Oszczypko *et al.*, 2006; Popadyuk *et al.*, 2006; Ślączka *et al.*, 2006; Pietsch *et al.*, 2010; Warchoł, 2011). Structural and sedimentological data suggest that the area has considerable potential for new discoveries through the use of modern exploration methods.

The Polish-Ukrainian, Carpathian Foredeep evolved from an intracratonic, Paratethyan basin that was cut off from the main Paratethys realm in the late Badenian (Oszczypko *et al.*, 2006; and references therein). As a result, evaporites formed (Peryt, 2006; and references therein) as an important unit for correlation in the basin. They are overlain by a succession of calcareous and siliciclastic molasse deposits (Vyalov, 1965; Oszczypko, 1996), with a thickness of up to 3 km in the Polish part (Ney *et al.*, 1974) and up to 6 km in the Ukrainian part of the basin (Oszczypko, 2006). Sedimentation was controlled by tectonics, regional climate and relative sea-level changes. Distinct zones of sedimentation are recognizable in the foredeep basin, with the Carpathian-derived, terrigenous sediment dominating the higher-relief southern part and with bioclastic limestones and northerly-derived, terrigenous sediment, deposited in the shallow-water, northern part of the basin (Wysocka, 2002). The deep, subneritic, axial zone of the basin was dominated by eastward-flowing turbidity currents.

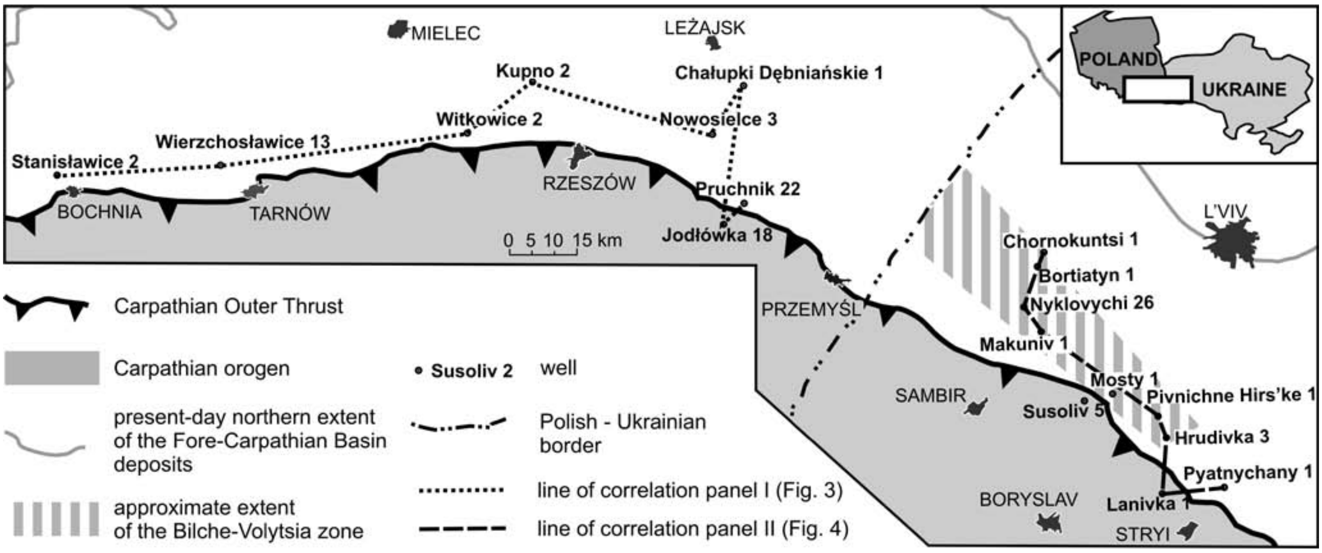

Fig. 1. Locality map of study area in relation to Carpathian, outer-thrust, orogenic front, with location of wells studied and lines of their correlation panels

The present study focussed on the middle Miocene depositional environments and their sedimentation patterns, associated with the southern margin of the Carpathian Foredeep, in the eastern part of the basin, which stretches across the Polish-Ukrainian border (Fig. 1). The research project was a result of co-operation between Polish and Ukrainian institutions, which provided a unique opportunity to extend the study area eastwards, by using well cores from both sides of the border. On the basis of cores, a sedimentary facies analysis of the mid-Miocene deposits was conducted, shedding light on their heterogeneity and yielding significant implications with regard to regional prospecting for hydrocarbon reservoirs.

GEOLOGICAL SETTING

The Carpathian Foredeep is the latest part of a peripheral foreland basin, formed in front of the Carpathian orogenic belt. The basement consists of various Proterozoic and Palaeozoic rocks of the European Platform, including its Mesozoic cover (Oszczypko *et al.*, 2006). The asymmetrical foreland basin developed by flexural basement subsidence in front of the Outer Carpathian Thrust in Eggenburgian–Sarmatian time (Oszczypko, 1996). The lithostratigraphic divisions of the basin-fill molasse succession in the Polish and Ukrainian parts of the basin are somewhat different, but broadly correlative (Fig. 2). A key marker unit is the Badenian evaporites (the Krzyżanowice Formation in Poland and the Tyras Formation in Ukraine), which correspond to the lower part of nannoplankton zone NN6 (Peryt, 1997, 1999).

Along the front of the Outer Carpathian Thrust (Fig. 1), there is a wide zone of folded, Miocene deposits, both in Ukraine and in Poland. These deposits form the Boryslav-Pokuttya and Sambir nappes in Ukraine and the Stebnik Nappe and Zgłobice imbricate thrust-sheets in Poland (Oszczypko *et al.*, 2006). The Stebnik Nappe is considered to be equivalent to the Sambir Nappe, whereas the exact, lateral extension of the Boryslav-Pokuttya Nappe in the Polish area remains unclear (Andreyeva-Grigorovich *et al.*, 2008). All the wells studied, except for Lanivka 1 and Jodłówka 18 (Fig. 1), are located outside this frontal fold-and-thrust belt. The Polish wells are in the eastern part of the Polish Carpathian Foredeep and the Ukrainian wells are in the so-called Bilche-Volytsia Zone (Figs 1 and 2).

STUDY MATERIAL AND METHODS

Cores from eight wells were analysed in the Polish part of the study area: the Pruchnik 22, Jodłówka 18, Kupno 2, Stanisławice 2, Witkowice 2, Nowosielce 3, Chałupki Dębniańskie 1 and Wierzchosławice 13 wells, with a total of 194 m of well cores logged (Fig. 3). In addition, cores from ten wells in the Ukrainian part were studied: the Chornokuntsi 1, Bortiatyn 1, Nyklovychi 26, Makuniv 1, Mosty 1, Susoliv 5, Pivnichne Hirs'ke 1, Hrudivka 3, Pyatnychany 1 and Lanivka 1 wells, with a total of 519 m of cores logged (Fig. 4). Unfortunately, the Ukrainian cores were considerably poorer in quality, owing to their storage in unsuitable conditions.

Conventional methods of stratigraphic logging and standard, descriptive, sedimentological terminology were used (Harms *et al.*, 1975; Reineck & Singh, 1975; Collinson & Thompson, 1982), paying particular attention to such features as grain size, colour, and primary and secondary sedimentary structures (including soft-sediment deformation), as well as the occurrence of organic matter, intraformational clasts and pronounced calcite cementation. Sedimentary facies were defined as the main types of deposits, distinguished on such a descriptive basis, with a thickness resolution of ~5 cm adopted in the present study. Thin (1–3 cm) layers of massive or laminated siltstone or sandstone, intercalated with mudstone, were considered to be components of a heterolithic deposit, which as a whole might be mud-

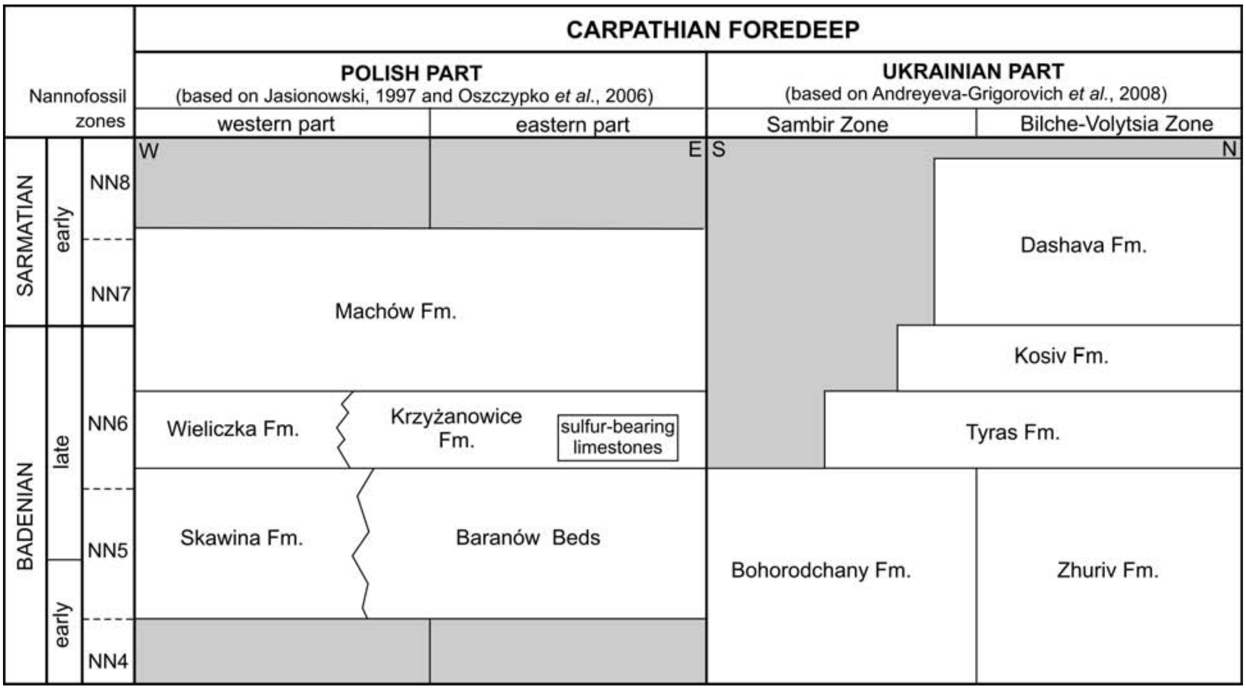

Fig. 2. Tentative correlation of Miocene, lithostratigraphic units in Polish and Ukrainian parts of Carpathian Foredeep (based on Andreyeva-Grigorovich *et al.*, 1997; Jasionowski, 1997; and Oszczypko *et al.*, 2006)

stone- or sandstone-dominated. For easier reference in the text and figures, facies have been labelled with the modified letter code of Eyles *et al.* (1983).

The quantitative method of embedded Markov-chain analysis (Gingerich, 1969; Krumbein & Dacey, 1969) was used for recognition of preferential trends in vertical facies organization, with an improved, statistical test (Harper, 1984) for the significance of the observed frequency of vertical facies transitions.

MIDDLE MIOCENE FACIES

Fourteen sedimentary facies have been distinguished in the well cores of the middle Miocene deposits in the Polish and Ukrainian parts of the study area. The facies, with their key characteristics and brief interpretation, are listed in Table 1 to give an overview. They are illustrated with core-sample photographs in Figure 5, and are further described and interpreted in detail in the present section. The stratigraphic distribution of facies in the main well logs is shown in Figures 6 and 7.

Facies Sm: massive sandstones

Description. These sandstones are whitish-grey, fine- to medium-grained and massive, with no recognizable, internal stratification (see Sm in Fig. 5). Their beds have sharp bases and either sharp or gradational tops and occur in both the Polish (Fig. 6) and the Ukrainian wells (Fig. 7), but seem to be most common in the Polish Jodłówka 18 well (Fig. 3). Bed thickness ranges from a few centimetres to 2.5 m (e.g., see well log Jodłówka 18 in Fig. 6, depth 2104.5–2107 m). The beds lack any systematic, internal grain-size grading, although some of the thicker ones show a subtle, upward coarsening at the base and/or slight, upward fining at the top. Many beds contain scattered fragments of bivalve shells, carbonaceous plant detritus and abundant muscovite flakes. Mudstone intraclasts occur in this sandstone facies in the Nowosielce 3 well (Fig. 3, well depth 1173 m). However, this sandstone facies is generally arenitic and contains little or no disseminated mud matrix.

Interpretation. The lack of internal stratification and bed-scale, normal grading precludes the possibility of deposition from turbulent flow and indicates sand emplacement by a cohesionless debris flow in the frictional regime of Drake (1990). Basal, inverse grading indicates intense grain collisions at the base of self-lubricated shearing flow (Campbell, 1989), whereas the normal-graded bed tops reflect the interaction of shearing flow with the overlying ambient water (Middleton & Southard, 1978). The arenitic texture and the occurrence of plant detritus and bivalve shells indicate submarine resedimentation of river-derived sand, which most likely would occur on the slopes of shelf-margin deltas (Porębski *et al.*, 2002; Porębski & Steel, 2003). The thicker, massive beds probably represent large delta-slope failures, whereas the thinner ones may be due to secondary collapsing of the steep snouts of "frozen" debris flows or to secondary, gravitational sloughing of the slope-scar head scarps, left by large, gravitational failures.

Facies Sng: normal-graded sandstones

Description. These sandstone are whitish-grey to light grey, fine- to medium-grained and non-stratified (massive), but their beds show normal grading and occasionally also

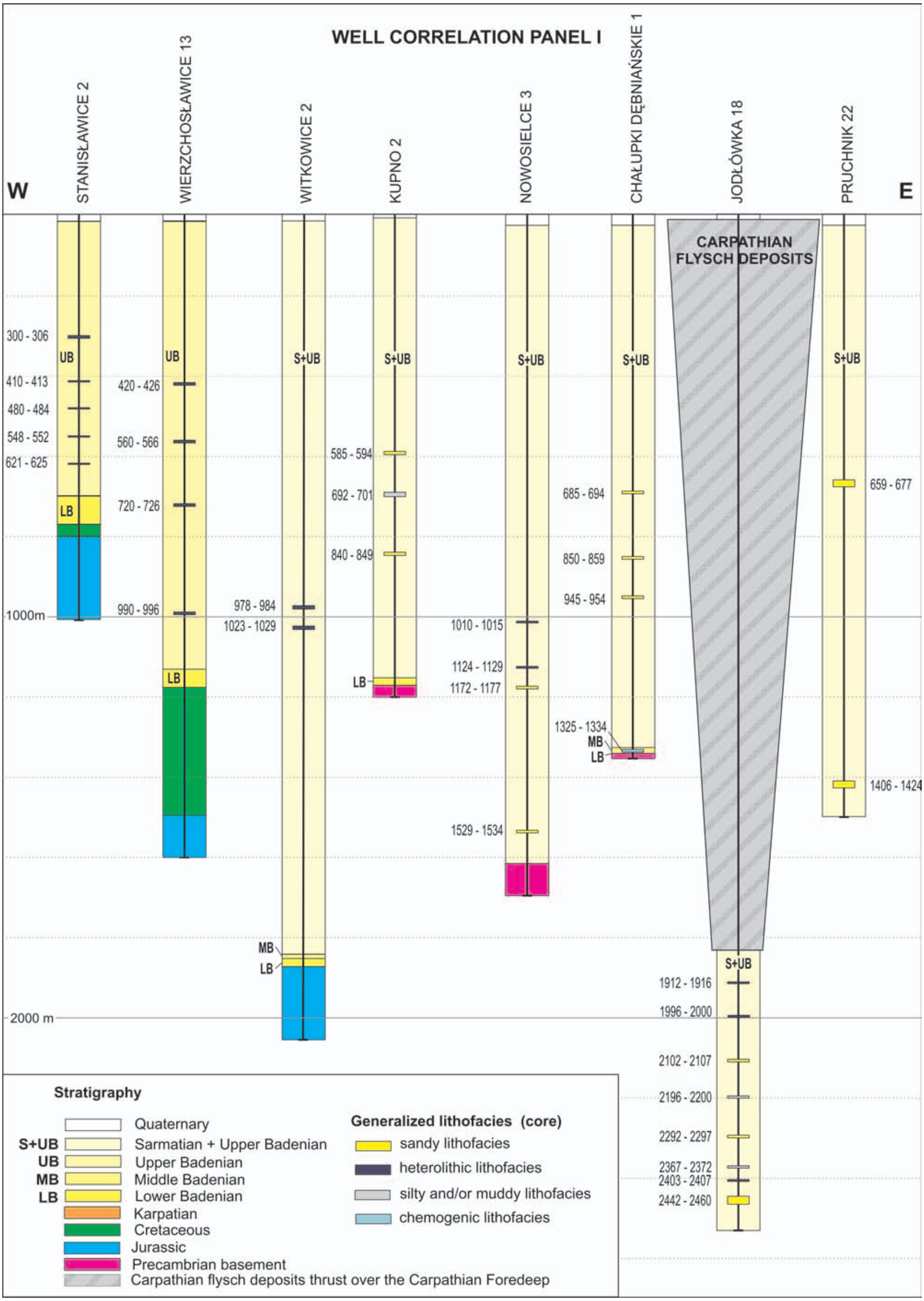

Fig. 3. Well-log correlation panel for Polish part of Carpathian Foredeep (see well location and correlation line in Fig. 1)

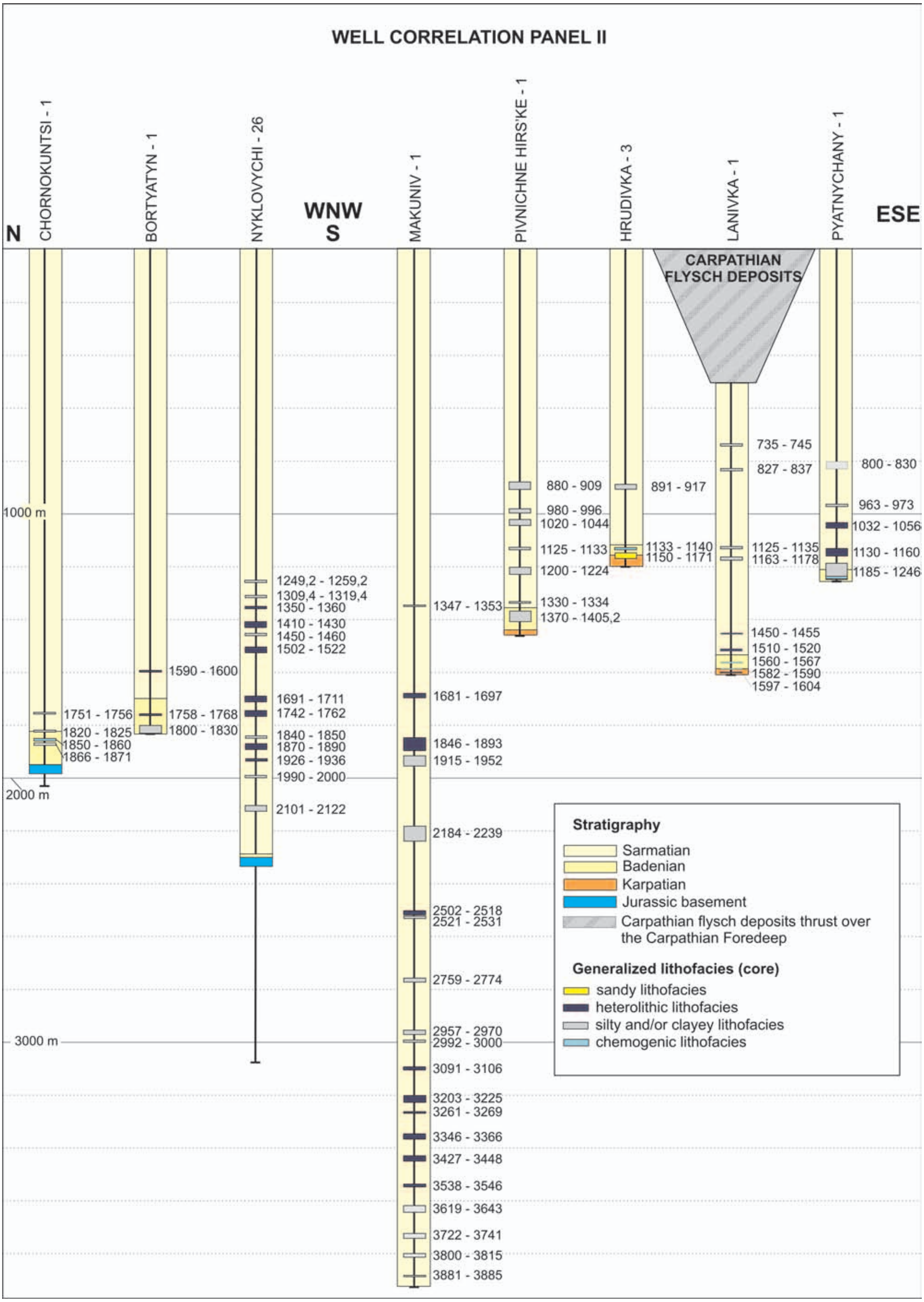

Fig. 4. Well-log correlation panel for Ukrainian part of Carpathian Foredeep (see well location and correlation line in Fig. 1)

Table 1

Sedimentary facies, distinguished in middle Miocene, basin-fill succession, with their key, descriptive features and brief, genetic interpretation (for details, see text)

FACIES CODE	FACIES	MAIN FEATURES	THICKNESS [cm]	DEPOSITIONAL MECHANISM
Sm	Massive sandstone	no stratification or normal grading	5–140	debris flow
Sng	Normal-graded massive to stratified sandstone	normal grading	10–70	turbulent high-density flow (HDTC)
Sd	Deformed sandstone with sporadic intraclasts	intense soft-sediment deformation	10–20	slumping
Sh	Planar parallel-stratified sandstone	plane-parallel stratification	8–80	plane-bed transport by waves with high orbital velocities or by tractional current in upper flow regime*
St	Trough cross-stratified sandstone	trough cross-stratification	30–35	SCS or dune transport by current in upper range of lower flow regime
Sr	Ripple cross-laminated sandstone, locally deformed	ripple cross-lamination	4–85	ripple transport by waves with low orbital velocieties or by tractional current in lower range of lower flow regime*
$H_{S>F}$	Sandstone-dominated heterolithic deposits	flaser bedding	10–225	weak tractional current alternating with minor mud-suspension fallout
$H_{S\approx F}$	Sandstone-mudstone heterolithic deposits	wavy bedding	15–40	weak tractional current alternating with major mud-suspension fallout
$H_{F>S}$	Mudstone-dominated heterolithic deposits	lenticular bedding	8–470	mud-suspension fallout alternating with sand-starved weak current
Fm	Massive mudstone	no structures	2–290	hemipelagic suspension fallout*
Fl	Laminated mudstone	flat parallel lamination	40–900	pulsating or weak current-driven fallout of hemipelagic suspension*
FE	Mudstones interlayered with gypsum and anhydrites	flat lamination	?	mud-suspension fallout with sporadic evaporitic precipitation
EF	Gypsum and anhydrites interlayered with mudstones	flat lamination	120–500	evaporitic precipitation alternating with mud-suspension fallout
E	Gypsum and anhydrites	occasional nodular structures	280	evaporitic precipitation

*May form divisions of turbidite deposited by LDTC

planar, parallel stratification at the top. This facies occurs mainly in the Polish wells. Beds are 10 to 70 cm thick and most commonly show consistent, normal grading (e.g., the Kupno 2 well in Fig. 6, depth 586 m). Basal, inverse grading is less common (e.g., well log Chałupki Dębniańskie 1 in Fig. 6, depth 687.7 m), whereas pensymmetric or symmetric, inverse-to-normal grading is rare (e.g., well log Chałupki Dębniańskie 1 in Fig. 6, depths 688.8 and 855.5 m). Some beds contain mudstone intraclasts, fragments of coalified plant matter and/or abundant muscovite flakes.

Interpretation. The normal-graded massive beds with or without a parallel-stratified top part indicate deposition by rapid dumping from an excessively concentrated turbulent suspension (Lowe, 1988), often followed by a tractional phase of plane-bed transport. These beds in a submarine setting would be neritic or subneritic turbidites Ta(b) (Bouma, 1962; Allen, 1991), attributed to high-density turbidity currents (*sensu* Lowe, 1982), or a variety of tempestites, emplaced in sublittoral environment (Myrow & Southard, 1991, 1996). A relatively thin (≤ 10 cm) basal zone of inverse grading may represent turbiditic traction carpet (Lowe, 1982; Hiscott, 1994). Beds with a thicker inversely-graded lower part are attributed to high-density turbidity currents, generated by the retrogressive slumping of a delta slope, where the first-mobilized, lower-slope sediment would be finer-grained than the subsequently mobilized sediment of a higher slope. The head part of the turbidity current in such a case then would carry a finer-grained load than that carried by the flow body. Alternatively, the upward increase in grain size may reflect waxing of a delta-derived, hyperpycnal flow (Kneller & Branney, 1995; Parsons *et al.*, 2001) or a storm-generated, seaward relaxation current (Myrow & Southard, 1991).

Facies Sd: hydroplastically deformed sandstones

Description. These sandstones range from fine- to medium/coarse-grained, are grey to light-grey in colour and show hydroplastically deformed, internal, parallel stratification and/or ripple cross-lamination (see Sd in Fig. 5). Bed thicknesses are in the range of 4 to 20 cm and at least the upper bed boundaries are generally sharp. Some of the sandstone beds contain scattered mudstone intraclasts, typically rounded in shape and from 0.5 cm (e.g., well log Pruchnik 22 in Fig. 6, depth 668 m) to 6 cm in size (e.g., the Jodłówka 18 well in Fig. 3, depth 2449.5 m).

Interpretation. All the thin beds of this facies were convoluted *in situ* by such factors as sediment loading, partial liquefaction, caused by a seismic tremor or an overpassing bottom current (Dżułyński & Walton, 1965), and in some cases by bioturbation (e.g., see Sd in Fig. 5) However, at least some of the thicker and sharp-based beds may repre-

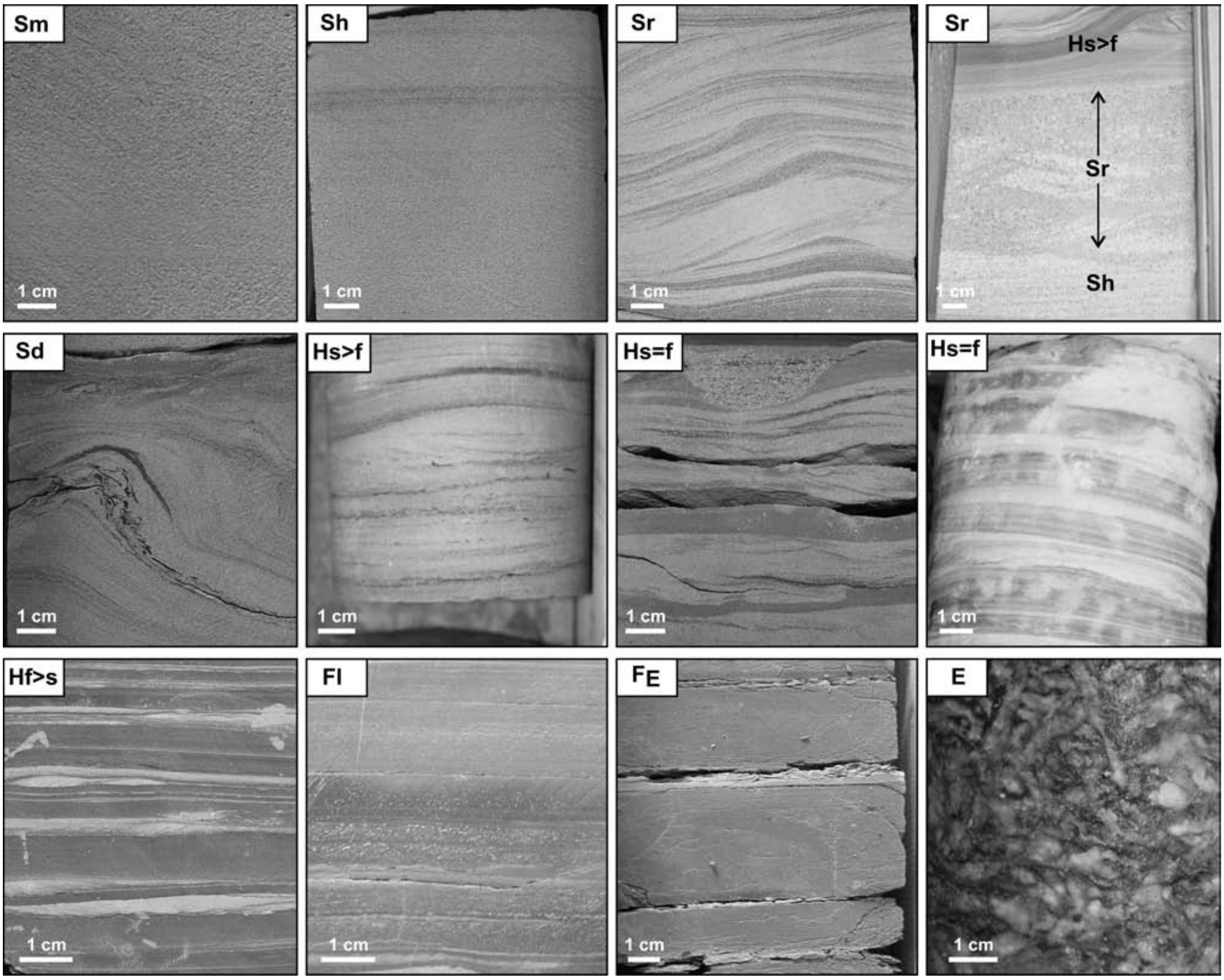

Fig. 5. Well-core photographs, showing main, sedimentary facies, distinguished in mid-Miocene succession studied; facies letter code, as given in Table 1 and used in text

sent local intra-slope slumps, caused by an excess accumulation of terrigenous sediment on the basin-margin, gentle, neritic slope (Lewis, 1971).

Facies Sh: planar-parallel-stratified sandstones

Description. These sandstones range from very fine- to medium-grained, are light-grey to grey in colour and characterized by planar parallel stratification, horizontal or slightly inclined (see Sh in Fig. 5). Stratification is marked by subtle changes in grain size and/or colour. Bed thicknesses are from a few centimetres to 80 cm (e.g., well log Pruchnik 22 in Fig. 6, depth 668 m). Mudstone intraclasts and coalfield plant detritus are rare (e.g., found in the Jodłówka 18 well, depth 2403.5 m; Fig. 3).

Interpretation. This facies is attributed to the plane-bed transport of sand by a unidirectional current in the upper flow regime (Allen, 1968; Harms *et al.*, 1975) or by waves with relatively high, orbital velocities (Komar & Miller, 1975; Komar, 1998). The so-called lower stage, plane-bed transport can be precluded, as it would require at least coarse sand (grain size >0.7 mm). Inclined, planar-parallel stratification is typically due to the plane-bed transport of sand over a non-horizontal surface, such as a gentle scour, formed by a current, an erosional substrate truncation by storm waves, or a pre-existing, low-relief, depositional topography (e.g., delta-slope mounds or storm-emplaced shoreface sand patches).

Facies St: trough-cross-stratified sandstones

Description. The sandstones of this facies are fine- and medium-grained and light grey in colour, characterized by trough cross-stratification. Their concave-upwards sets of tangential strata are 7–10 cm thick, occurring isolated in association with the previous facies (Sh) or forming cross-strata cosets, up to 30 cm thick (as found only in the Pruchnik 22 well at depths 670.5 and 1422.5 m; Fig. 6).

Interpretation. The sporadic isolated trough cross-strata sets are thought to be scour-and-fill features, the association of which with facies Sh suggests swaley cross-stratification and thus episodic, storm-generated conditions, combining unidirectional currents and waves (Dumas & Arnott, 2006). The cosets of trough cross-strata indicate the migration of small dunes, which implies deposition by a unidirectional current in the upper range of the lower flow regime (Harms *et al.*, 1975). For the dunes to form, the current could not have been a brief surge and was probably a delta-derived, hyperpycnal flow, perhaps slightly channelized or conveyed by a delta-slope chute (Nemec, 1990; Parsons *et al.*, 2001).

Facies Sr: ripple-cross-laminated sandstones

Description. These sandstones are light grey, range from very fine- to medium-grained and show ripple cross-lamination. Well-core samples do not allow in all cases a clear distinction between current- and wave-ripple cross-lamination. The cross-laminae sets in the present case indicate mainly asymmetrical ripples, often climbing at an angle of 10–70° and occasionally deformed, but neither of these features is discriminative (Allen, 1968; Collinson & Thompson, 1982). Therefore, this sandstone facies includes both varieties of ripple cross-lamination. These sandstones occur in most wells and their beds vary in thickness from a few centimetres to 40 cm (e.g., well-log Pruchnik 22, depth 663 m; Fig. 6). The bed bases are generally sharp, but their tops often show the ripple-form relief preserved, particularly when covered by mudstone facies.

Interpretation. This facies represents sand deposition from a unidirectional current with flow power in the lower range of the lower flow regime (Allen, 1968; Harms *et al.*, 1975) or by waves with relatively low, orbital velocities (Komar & Miller, 1975; Komar, 1998). The climbing of ripples in either case would indicate a high rate of sand fall-out from suspension, relative to the rate of lateral transport in bedload traction (Allen, 1968). Sporadic deformation may be due to the shearing action of an overpassing current, stronger wave strokes, bioturbation or spontaneous, partial liquefaction.

Facies H: heterolithic deposits

Description. These deposits consist of light-grey sandstone and grey siltstone, thinly interbedded with dark-grey mudstone. The proportion of sandstone and siltstone to mudstone by thickness varies and accordingly the deposits have been categorized as three heterolithic facies (Table 1): facies $H_{S>F}$, dominated by sandstone and siltstone; facies $H_{S\approx F}$, with an approximately equal proportion of sandstone/siltstone and mudstone; and facies $H_{F>S}$, dominated by mudstone.

Facies $H_{S>F}$ (see in Fig. 5) occurs in most of the wells (Figs 6 and 7). Its coarser-grained component ranges from siltstone to medium-grained sandstone and is commonly cross-laminated. Bidirectional cross-lamination and subhorizontal, erosional truncations are common. Mudstone forms thin, discontinuous flasers (simple or bifurcated) and subordinate, continuous, undulating, wavy interlayers (wavy bedding *sensu* Reineck & Singh, 1975). Mud-flame load features, loaded ripples and pseudonodules (Dżułyński & Walton, 1965) are common. The units of this facies are 1–9 m thick (e.g., see well log Pruchnik 22, depth 1413–1422 m, Fig. 6), most often alternating with units of the other heterolithic facies.

Facies $H_{S\approx F}$ (see in Fig. 5) similarly occurs in most of the wells (Figs 6 and 7). Its coarser-grained component is predominantly very fine- to fine-grained sandstone, mainly cross-laminated. Bidirectional cross-lamination and erosional truncations are common. Mudstone forms comparably thick, continuous and undulating wavy interlayers (wavy bedding *sensu* Reineck & Singh, 1975). The units of this facies are mainly 50–70 cm thick, but locally reach 3 m (the Jodłówka 18 well, depth 2404–2407 m, Fig. 6), and are alternating with the other heterolithic facies.

Facies $H_{F>S}$ (see in Fig. 5) also occurs in most of the wells (Figs 6 and 7). It is dominated by mudstone, and its coarser-grained component forms mainly lenses of siltstone and very fine- to fine-grained sandstone (lenticular bedding *sensu* Reineck & Singh, 1975), although some sandstone interlayers are laterally more continuous and mudstone locally is reduced to flasers. Loaded ripples and pseudonodules are common. The units of this facies are mainly about 1 m in thickness, alternating with the other, heterolithic facies.

Interpretation. The alternation of sandstone/siltstone and mudstone and the evidence of bidirectional cross-lamination are diagnostic of a tidal environment (Reineck & Singh, 1975), which in the present case is ascribed to inter-deltaic, nearshore embayments, sheltered from wave action. No evidence of coastal barriers was recognized, which renders tidal lagoons a less likely, alternative interpretation. Facies $H_{S>F}$, $H_{S\leq F}$ and $H_{F>S}$ thus would represent sandflat, mixed-flat and mudflat, tidal environments, respectively (Reineck & Singh, 1975). The stratigraphic alternation of these facies reflects variable, local delivery of silt and sand, which may be due to the tidal environment's autogenic changes in sediment-dispersal pattern or may possibly reflect minor changes in relative sea level.

Facies F: mudstones

Description. These deposits are dark grey to blackish grey mudstones, which are common in all of the well cores studied (Figs 6 and 7) and range from massive (facies Fm) to laminated (facie Fl). The latter facies is characterized by an alternation of darker and lighter grey, thin bands, 3–5 mm in thickness (see Fl in Fig. 5), which apparently reflects variable proportions of the clay and silt fractions. Vertical and horizontal burrows occur sporadically.

Interpretation. The origin of this facies is attributed to the fall-out of hemipelagic mud suspensions, derived mainly by storms, hyperpycnal flows and other turbidity currents. The banded mudstones of facies Fl probably owe their origin to a pulsating, seaward delivery of muddy suspension by storms and delta-derived, hypopycnal plumes (Nemec, 1995).

Facies E: evaporites

Description. This facies consists of whitish to light grey evaporites, chiefly gypsum alternating with anhydrite. The anhydrite is nodular or laminated, whereas gypsum has a coarse-crystalline texture. Some depositional units are composed solely of evaporites (facies E, see Fig. 5), whereas other evaporitic units are thinly interlayered with subordinate mudstone (facies E_F, see Fig. 5) or virtually dominated by the latter (facies F_E). The inter-evaporitic mudstone layers are dark grey and 1–5 mm in thickness. The units of facies E_F encountered by the wells (Figs 6 and 7) are 120–500 cm thick. Only one unit of facies E (~2.8 m thick) and one unit of facies F_E (>15 m thick, not drilled to its base) were encountered by the well. These evaporitic facies are found in the deepest parts of the wells (see the well logs Chałupki Dębniańskie 1 in Fig. 6 and Hrudivka 3, Lanivka 1 and Pyatnychany 1 in Fig. 7).

Interpretation. These evaporitic deposits represent the Badenian Krzyżanowice Formation in Poland and the coeval Tyras Formation in Ukraine (Fig. 2), which are the shallow-marine substrate, predating the late Badenian, flexural subsidence of the foredeep basin. The depositional conditions of the evaporites have been discussed by Peryt (1997, 1999), among other authors. The precipitation of gypsum and anhydrite occurred probably in coastal sabkhas or shallow, marine embayments, isolated from the Paratethian Sea domain by the foreland uplift. The differing, volumetric proportion of the mudstone component in facies E, E_F and F_E reflects the variable degree of storm, tidal and deltaic influence in these protected shoal-water environments.

VERTICAL FACIES ORGANIZATION

The individual sedimentary facies (Table 1) differ markedly in texture and depositional structures, which obviously has a bearing on their internal porosity and permeability properties and is arguably the main source of the primary heterogeneity of the sedimentary succession (e.g., see Weber, 1982, 1986). The vertical facies transitions in well logs have thus been studied on a statistical basis, with the use of Markov-chain analysis, in order to recognize the pattern of vertical facies organization in the study area. The role of secondary heterogeneities, related to faults and/or differential cementation, is not considered here and should be a subject for a separate study.

The results of Markov-chain analysis are shown in the form of numerical matrices in Figure 8. The vertical facies transitions that appear to be more frequent than random (see the positive values in matrix D; Fig. 8) are displayed in Figure 9A, which thus reveals an overall pattern of high-frequency, vertical facies changes within the mid-Miocene sedimentary succession of the study area. In metric terms, these frequencies can be scaled further, using the thickness range of the individual facies (Table 1). The porosity and permeability properties of the individual facies, once determined by a laboratory study, can be attached readily to the facies organization model.

The statistically preferential trend of vertical facies transitions, revealed by the Harper (1984) test (Fig. 8E), is shown in Figure 9B and its interpretation is given in Figure 10. There seem to be four different modalities in the vertical organization of facies, representing the following four main, sedimentary environments (Fig. 10):

(1) A shoal-water evaporitic environment, with alternation of facies E and E_F (Fig. 9B), which formed prior to the late Badenian ultimate phase of foredeep development;

(2) A littoral, tidal environment (probably the inner parts of open bays, coastal, tidal flats and/or spit-sheltered, aerated lagoons), where the deposition of "domestic", heterolithic facies $H_{S>F}$, $H_{S\approx F}$ and $H_{F>S}$ was frequently interrupted by the storm emplacement of facies Sm;

(3) A littoral, wave-dominated, sandy environment, probably a shoreface zone, where wave-worked facies Sr and Sh alternated with each other, according to the varying, orbital velocity of sea waves;

(4) A neritic to subneritic, muddy, offshore slope environment, frequently invaded by sandy tempestites Sh-Sr in its shallower part and by surge-type turbidites Tad/Tbcd and hyperpycnites Tbcbc…d in the deeper part.

The one-directional, upward transition of the environmental modalities 1, 2 and 3 into modality 4 (Fig. 10) indicate their cessation by marine drowning, which probably reflects tectonically-induced, relative sea-level rises at the inner foredeep margin.

The preferential, vertical facies transitions and environmental modality changes revealed by the statistical analysis (Fig. 10) may serve as a useful, tentative guide for regional hydrocarbon-reservoir prospecting. The environmental modality 3, with its wave-worked sandstone facies, is the most promising as a potential hydrocarbon reservoir. Modality 4 involves sandstone beds, separated by mudstone caps, but the isolated sandstone tempestites and turbidites/hyperpycnites may be laterally extensive and volumetrically attractive as a potential reservoir type. The heterolithic modality 2 (Fig. 10) is much less attractive, although many, heterolithic reservoirs of this type have been produced successfully (Martinius *et al.*, 2005; Nordahl *et al.*, 2005; Ringrose *et al.*, 2005), provided that the initial reservoir pressure is sufficiently high and the production wells are well planned. The least attractive is facies modality 1 (Fig. 10), which includes no potential reservoir rocks and is practically a permeability barrier. However, this apparent barrier is broken by numerous, minor thrusts and younger, normal faults, which provide good connections with the deeper-buried, potential hydrocarbon source rocks.

Importantly, the statistical model of vertical facies transitions (Fig. 10) supports the notion that the southern zone of the Carpathian Foredeep basin evolved through episodes of tectonically-induced marine drowning and subsequent shoreline progradation. This means that a mudstone-rich, neritic facies assemblage, encountered in an exploration well, may signal an occurrence of a more promising sandy, littoral facies assemblage, directly below.

DEPOSITIONAL PALAEOENVIRONMENT

The interpretive facies analysis (Table 1) and recognition of facies vertical-organization modalities (Figs 9B and 10) shed more light on the depositional environment of the latest Badenian–early Sarmatian Machów Formation and its Ukrainian stratigraphic counterparts (Fig. 2). Prior to its flexural, tectonic roll-back that accommodated this thick sedimentary molasse succession, the Polish-Ukrainian foredeep was a shallow-water, evaporitic basin (facies modality 1 in Fig. 10). The late Badenian tectonic down-warping tur-

Facies	Sm	Sng	Sd	Sh	St	Sr	$H_{S>F}$	$H_{S\sim F}$	$H_{F>S}$	Fm	Fl	E	E_F
Sm		4	0	16	1	13	8	6	5	28	1	0	0
Sng	1		0	0	0	3	1	1	1	2	0	0	0
Sd	0	0		0	0	1	0	0	0	1	0	0	0
Sh	8	3	1		1	36	2	2	1	14	0	0	0
St	1	0	0	0		1	0	0	0	1	0	0	0
Sr	14	1	1	21	1		9	4	2	24	0	0	0
$H_{S>F}$	9	0	0	7	0	5		0	0	3	0	0	0
$H_{S\sim F}$	6	0	0	4	0	2	0		1	2	0	0	0
$H_{F>S}$	5	0	0	0	0	2	2	0		1	0	0	0
Fm	33	1	0	17	0	15	3	1	1		3	0	0
Fl	3	0	0	0	0	0	0	0	0	0		0	0
E	0	0	0	0	0	0	0	0	0	0	0		1
E_F	1	0	0	0	0	0	0	0	0	0	0	1	**A**

Facies	Sm	Sng	Sd	Sh	St	Sr	$H_{S>F}$	$H_{S\sim F}$	$H_{F>S}$	Fm	Fl	E	E_F
Sm		0.0488	0	0.1951	0.0122	0.1585	0.0976	0.0732	0.061	0.3415	0.0122	0	0
Sng	0.1111		0	0	0	0.3333	0.1111	0.1111	0.1111	0.2222	0	0	0
Sd	0	0		0	0	0.5	0	0	0	0.5	0	0	0
Sh	0.1176	0.0441	0.0147		0.0147	0.5294	0.0294	0.0294	0.0147	0.2059	0	0	0
St	0.3333	0	0	0		0.3333	0	0	0	0.3333	0	0	0
Sr	0.1818	0.013	0.013	0.2727	0.013		0.1169	0.0519	0.026	0.3117	0	0	0
$H_{S>F}$	0.375	0	0	0.2917	0	0.2083		0	0	0.125	0	0	0
$H_{S\sim F}$	0.4	0	0	0.2667	0	0.1333	0		0.0667	0.1333	0	0	0
$H_{F>S}$	0.5	0	0	0	0	0.2	0.2	0		0.1	0	0	0
Fm	0.4459	0.0135	0	0.2297	0	0.2027	0.0405	0.0135	0.0135		0.0405	0	0
Fl	1	0	0	0	0	0	0	0	0	0		0	0
E	0	0	0	0	0	0	0	0	0	0	0		1
E_F	0.5	0	0	0	0	0	0	0	0	0	0	0.5	**B**

Facies	Sm	Sng	Sd	Sh	St	Sr	$H_{S>F}$	$H_{S\sim F}$	$H_{F>S}$	Fm	Fl	E	E_F
Sm		0.0311	0.0069	0.2249	0.0104	0.2699	0.0865	0.0484	0.0381	0.263	0.0138	0.0035	0.0035
Sng	0.2244		0.0055	0.1801	0.0083	0.2161	0.0693	0.0388	0.0305	0.2105	0.0111	0.0028	0.0028
Sd	0.2201	0.0245		0.1766	0.0082	0.212	0.0679	0.038	0.0299	0.2065	0.0109	0.0027	0.0027
Sh	0.2656	0.0295	0.0066		0.0098	0.2557	0.082	0.0459	0.0361	0.2492	0.0131	0.0033	0.0033
St	0.2207	0.0245	0.0054	0.1771		0.2125	0.0681	0.0381	0.03	0.2071	0.0109	0.0027	0.0027
Sr	0.2774	0.0308	0.0068	0.2226	0.0103		0.0856	0.0479	0.0377	0.2603	0.0137	0.0034	0.0034
$H_{S>F}$	0.2348	0.0261	0.0058	0.1884	0.0087	0.2261		0.0406	0.0319	0.2203	0.0116	0.0029	0.0029
$H_{S\sim F}$	0.2275	0.0253	0.0056	0.1826	0.0084	0.2191	0.0702		0.0309	0.2135	0.0112	0.0028	0.0028
$H_{F>S}$	0.2256	0.0251	0.0056	0.1811	0.0084	0.2173	0.0696	0.039		0.2117	0.0111	0.0028	0.0028
Fm	0.2755	0.0306	0.0068	0.2211	0.0102	0.2653	0.085	0.0476	0.0374		0.0136	0.0034	0.0034
Fl	0.2213	0.0246	0.0055	0.1776	0.0082	0.2131	0.0683	0.0383	0.0301	0.2077		0.0027	0.0027
E	0.2195	0.0244	0.0054	0.1762	0.0081	0.2114	0.0678	0.0379	0.0298	0.206	0.0108		0.0027
E_F	0.2195	0.0244	0.0054	0.1762	0.0081	0.2114	0.0678	0.0379	0.0298	0.206	0.0108	0.0027	**C**

Facies	Sm	Sng	Sd	Sh	St	Sr	$H_{S>F}$	$H_{S\sim F}$	$H_{F>S}$	Fm	Fl	E	E_F
Sm		0.0176	0.0069	-0.0298	0.0018	-0.1114	0.0111	0.0247	0.0229	0.0785	-0.0016	-0.0035	-0.0035
Sng	-0.1133		-0.0055	-0.1801	-0.0083	0.1173	0.0419	0.0723	0.0806	0.0117	-0.0111	-0.0028	-0.0028
Sd	-0.2201	-0.0245		-0.1766	-0.0082	0.288	-0.0679	-0.038	-0.0299	0.2935	-0.0109	-0.0027	-0.0027
Sh	-0.1479	0.0146	0.0081		0.0049	0.2737	-0.0526	-0.0165	-0.0214	-0.0433	-0.0131	-0.0033	-0.0033
St	0.1126	-0.0245	-0.0054	-0.1771		0.1208	-0.0681	-0.0381	-0.03	0.1262	-0.0109	-0.0027	-0.0027
Sr	-0.0956	-0.0178	0.0061	0.0501	0.0027		0.0313	0.004	-0.0117	0.0514	-0.0137	-0.0034	-0.0034
$H_{S>F}$	0.1402	-0.0261	-0.0058	0.1033	-0.0087	-0.0178		-0.0406	-0.0319	-0.0953	-0.0116	-0.0029	-0.0029
$H_{S\sim F}$	0.1725	-0.0253	-0.0056	0.0841	-0.0084	-0.0858	-0.0702		0.0358	-0.0801	-0.0112	-0.0028	-0.0028
$H_{F>S}$	0.2744	-0.0251	-0.0056	-0.1811	-0.0084	-0.0173	0.1304	-0.039		-0.1117	-0.0111	-0.0028	-0.0028
Fm	0.1704	-0.0171	-0.0068	0.0086	-0.0102	-0.0626	-0.0445	-0.0341	-0.0239		0.0269	-0.0034	-0.0034
Fl	0.7787	-0.0246	-0.0055	-0.1776	-0.0082	-0.2131	-0.0683	-0.0383	-0.0301	-0.2077		-0.0027	-0.0027
E	-0.2195	-0.0244	-0.0054	-0.1762	-0.0081	-0.2114	-0.0678	-0.0379	-0.0298	-0.206	-0.0108		0.9973
E_F	0.2805	-0.0244	-0.0054	-0.1762	-0.0081	-0.2114	-0.0678	-0.0379	-0.0298	-0.206	-0.0108	0.4973	**D**

Facies	Sm	Sng	Sd	Sh	St	Sr	$H_{S>F}$	$H_{S\sim F}$	$H_{F>S}$	Fm	Fl	E	E_F
Sm		0.2524	1		0.575		0.4157	0.2065	0.2025	0.0709			
Sng						0.305	0.4758	0.2995	0.2431	0.5949			
Sd						0.379				0.3704			
Sh		0.3251	0.3607		0.4894	1E-06							
St	0.5267					0.5117				0.5015			
Sr			0.4109	0.1775	0.5485		0.2117	0.5077		0.1834			
$H_{S>F}$	0.0881			0.1506									
$H_{S\sim F}$	0.1034			0.2875					0.3755				
$H_{F>S}$	0.0528						0.1505						
Fm	0.0012			0.474							0.0803		
Fl	0.0108												
E													0.0027
E_F	0.1999											0.0054	**E**

Fig. 8. Numerical results of Markov-chain analysis. Matrices: **A** – transition count matrix, **B** – probability matrix of observed transitions, **C** – probability matrix of expected random transitions, **D** – probability diference matrix) and related, statistical significance test (matrix **E**)

ned the basin into an asymmetric, synclinal trough (Fig. 11), shallower to the west, bounded by the Carpathian orogen front from the south and by the outer-foreland peripheral bulge from the north.

The basin's northern margin was a broad, littoral shelf, dominated by waves and influenced by tidal currents (Wysocka, 2002; Mastalerz *et al.*, 2006), with relatively little of its bioclastic calcareous sediment released to the deep-water, axial zone. The main sediment supply was from the narrow and tectonically unstable, southern shelf zone (Fig. 11), hosting deltas, separated by tide-dominated coastal embayments, and passing seawards into a wave-worked, sandy shoreface zone, swept by longshore currents (facies modalities 2 and 3, Fig. 10). The influence of tidal currents is well documented in the Miocene, western Paratethys (e.g., Sztano & De Boer, 1995). The adjacent, offshore environment was a neritic to subnaritic, muddy slope (Fig. 11), accumulating sandy tempestitites and conveying delta-derived, sand-laden turbidity currents (facies modality 4, Fig. 10) to the basin's deep zone. The turbidity currents included both brief, collapse-generated surge flows and river-generated, longer-duration, hyperpycnal flows (Porębski & Warchoł, 2006; Warchoł, 2011).

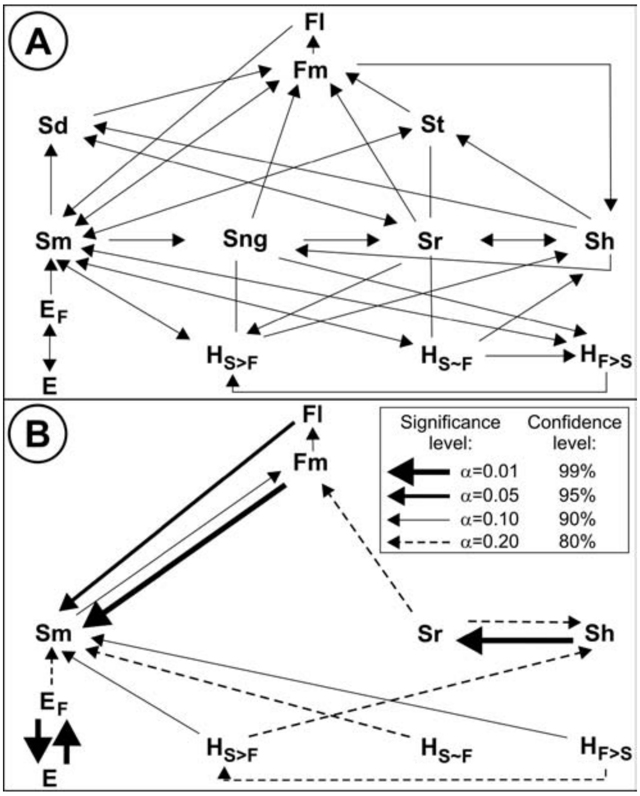

Fig. 9. Flow diagrams. **A** – vertical facies transitions that appear to be more frequent than random (see positive values in matrix D in Fig. 8). **B** – vertical facies transitions that have an occurrence probability > 80% according to statistical test (see values < 0.20 in matrix E, Fig. 8)

IMPLICATIONS FOR HYDROCARBON EXPLORATION

The source rocks for microbial gas in the Carpathian Foredeep are considered to be the Miocene claystones and mudstones (Kotarba *et al.*, 2011), which volumetrically dominate in the basin-fill sedimentary succession (e.g., Figs 6 and 7). They are intercalated abundantly with sandstones that act as hydrocarbon reservoirs. The main issue for hydrocarbon exploration in the basin is a detailed understanding of the paths of primary migration of gas from the source rocks into sandstones and its secondary migration within the sandstone bodies. Another crucial issue is the recognition of hydrocarbon traps, some of which may be far more difficult to recognize than others.

Structural traps. The evidence from seismic data, cores and geophysical well logs and well-production tests indicates that the most important reservoirs in the foredeep basin are structural traps, such as compactional anticlines, blind-thrust anticlines and thrust footwalls, as well as younger, extensional fault zones (Myśliwiec, 2004). Most of the hydrocarbon production thus far has been from compactional anticlines, which formed in the Miocene deposits in response to uneven bedrock morphology (i.e., Precambrian, Palaeozoic or Mesozoic rocks). Examples of such gas fields, related to local bedrock highs, are the Cetynia, Kamień, Jeżowe, multihorizon Jarosław, Kańczuga, Chałupki Dębniańskie and Jodłówka fields (Fig. 1). Gas fields related to the Carpathian thrusts are some of the largest in the Polish part of the basin, including the Przemyśl–Jaksmanice, Husów–Albigowa–Krasne and Pilzno fields (Karnkowski, 1999). The trap in such cases is formed by the thrust hanging-wall to the south and the water-gas contact to the north. The most difficult to recognize are traps, related to steep fault zones and exemplified by such gas fields as the Rudka, Ryszkowa Wola, Jarosław and Dzików fields (see Karnkowski, 1999). Two main regional systems of faults are recognized in the Carpathian Foredeep. The system of faults, trending NW–SE, is related to tectonic extension, caused by the latest approach and uplift of the Carpathian orogen (Krzywiec, 1999), and is considered to provide the main migration paths for hydrocarbons (Karnkowski, 1999). The associated system of transverse faults is thought to provide the gas-trapping seals (Karnkowski, 1999).

Stratigraphic traps. The other, main type of hydrocarbon trap in the Carpathian Foredeep is stratigraphic (Myśliwiec, 2004), although these are extremely difficult to indentify from seismic sections, owing to the resolution limit and have generally been underestimated in importance. The Miocene basin-fill succession consists of highly contrasting facies assemblages (Fig. 10), with the sandstone bodies, enveloped by and pinching out in muddy deposits, which gives increased potential for numerous, stratigraphic traps. On account of the great thickness of the sedimentary succession in the basin fill, (Figs 3 and 4), even small or "subtle" stratigraphic traps in total may contain large volumes of hydrocarbons. If correctly recognized and efficiently produced as groups, stratigraphic traps may be far more important than presently is believed.

However, the recognition of stratigraphic traps relies heavily on well data, particularly core samples, which allow

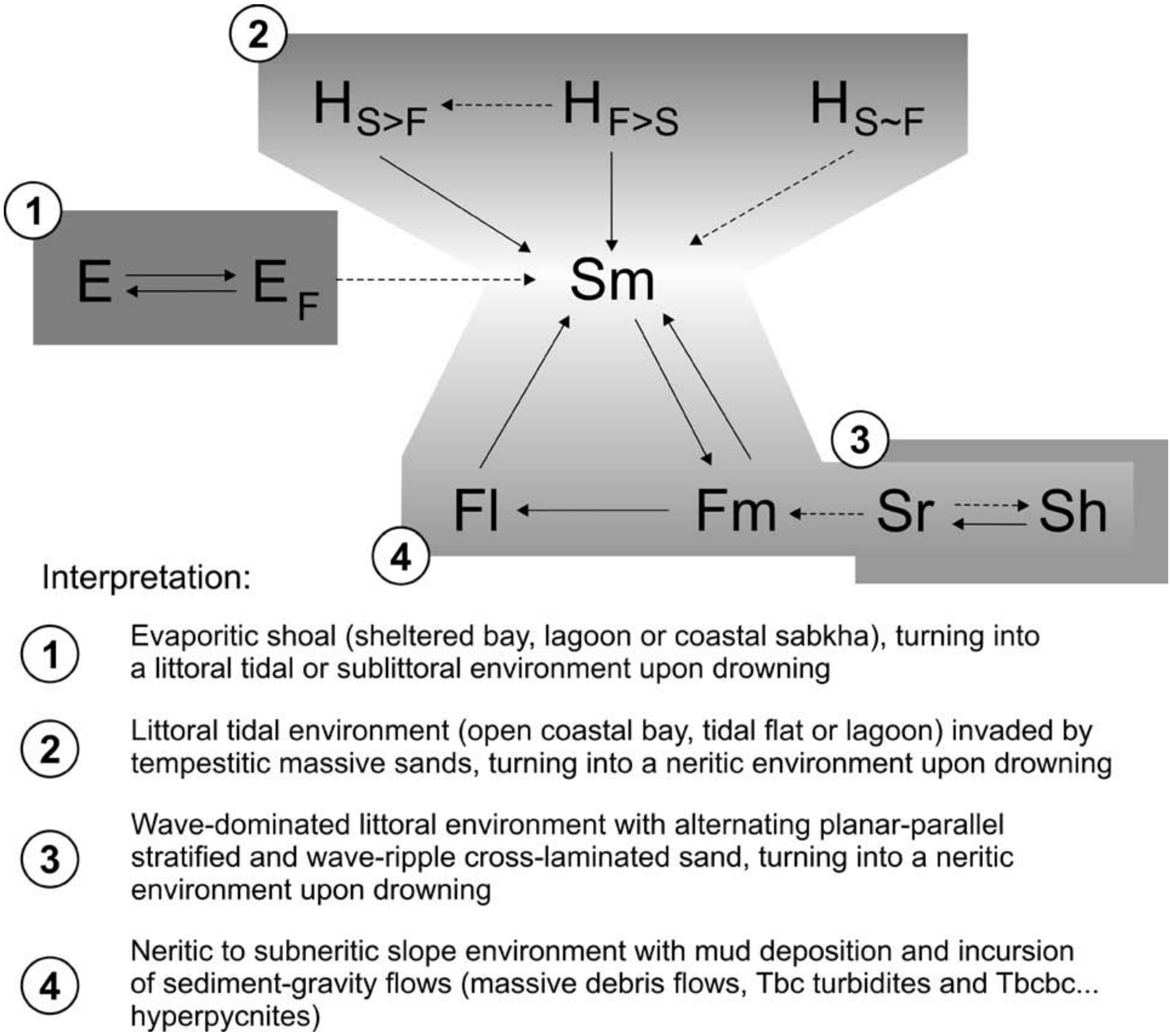

Fig. 10. Palaeoenvironmental interpretation of vertical, facies-transition modalities, revealed by Markov-chain analysis (Fig. 9B and matrix E in Fig. 8)

sedimentary facies to be identified and their spatial distribution to be predicted. In this respect, the sparse, "economic" coring, employed to date for wells drilled in the basin (e.g., see Figs 3 and 4), does not improve their sedimentological resolution by comparison with that of seismic sections, which is far below what might be regarded as optimum . It is crucial, therefore, that a number of fully cored wells be drilled in the most promising parts of the basin, recognized from seismic sections, in accordance with present-day practice in global petroleum exploration.

CONCLUSIONS

The present sedimentological study, based on well cores from the Polish and Ukrainian parts of the Carpathian Foredeep, revealed general facies heterogeneity in the middle Miocene sedimentary succession of the basin and recognized four main modalities of vertical facies organization. These different facies assemblages represent:

– the mid-late Badenian shoal-water evaporitic environment that preceded the latest Badenian–early Sarmatian main phase of foredeep development;

– a littoral, tidal environment, referable to the inner parts of storm-influenced, coastal bays and tidal flats and possibly some spit-sheltered lagoons;

– a littoral, wave-dominated, sandy environment, considered to be the shoreface zone, extended by waves in front of advancing deltas;

– a neritic to subneritic, muddy, offshore slope environment, with frequent incursions of tempestitic and turbi- ditic sand.

The study has contributed to a better understanding of the depositional systems of the foredeep basin and yielded significant implications for ongoing hydrocarbon exploration. The origin of potential reservoir sandstones was recognized, which also sheds light on their expected, stratigraphic occurrence in the basin-fill succession. The potential, economic importance of stratigraphic hydrocarbon traps was noted. In this context, the urgent need for full-scale facies analysis, with fully cored wells in strategic parts of the basin, was indicated.

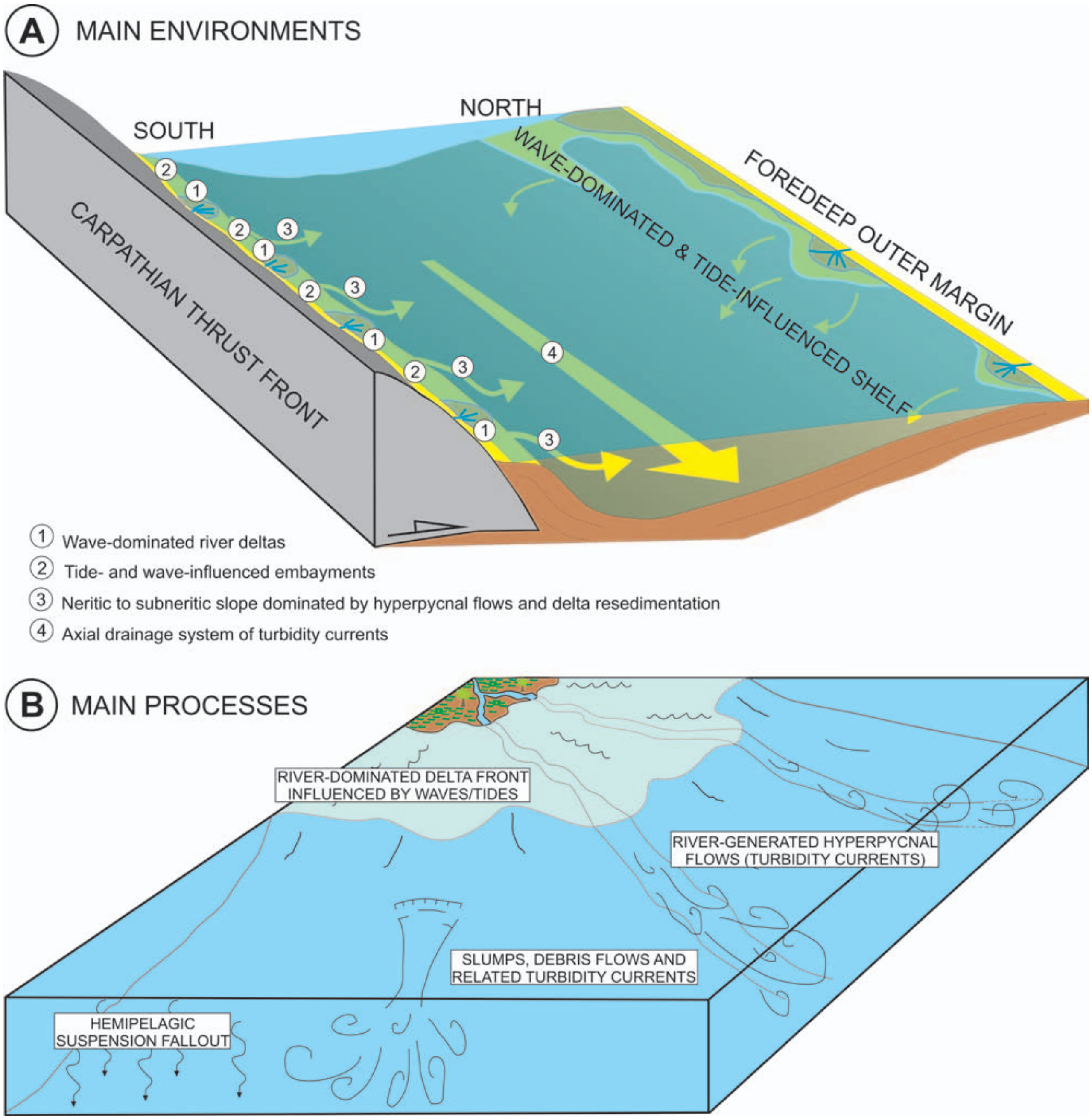

Fig. 11. Schematic, palaeoenvironmental model of mid-Miocene, Carpathian Foredeep (diagram not to scale), showing spatial distribution of main, sedimentary environments and principal, depositional processes involved. Processes and deposits discussed in present paper are associated with southern margin of basin

Acknowledgements

The study was conducted in 2007–2010 as a part of the research project UKRAINA/193/2006, financed by the Polish Ministry of Science and Higher Education and facilitated by the University of Science and Technology (AGH) in Kraków and the Polish Geological Institute in Warszawa. All the help, received from the Institute of Geology and Geochemistry of Combustible Minerals, Ukrainian National Academy of Science, in Lviv, is gratefully acknowledged.

Cordial thanks are offered to the reviewers, Szczepan Porębski (University of Science and Technology, Kraków) and ASGP editor Wojciech Nemec, whose constructive comments and critical remarks have improved and enriched this paper.

REFERENCES

Allen, J. R. L., 1968. *Current Ripples and Their Relation to Patterns of Water Flow and Sediment Motion*. North Holland, Amsterdam, 433 pp.

Allen, J. R. L. 1991. The Bouma division A and the possible duration of turbidity currents. *Journal of Sedimentary Research*, 61: 291–295.

Andreyeva-Grigorovich, A. S., Oszczypko, N., Ślączka, A., Oszczypko-Clowes, M., Savitskaya, N. & Trofimovicz, N., 2008. New data on the stratigraphy of the folded Miocene Zone at the front of the Ukrainian Outer Carpathians. *Acta Geologica Polonica*, 58: 323–353.

Bouma, A. H., 1962. *Sedimentology of Some Flysch Deposits: A*

Graphic Approach to Facies Interpretations. Elsevier, Amsterdam, 168 pp.

Campbell, C. S., 1989. Self-lubrication of long runout landslides. *Journal of Geology*, 97: 653–665

Collinson, J. D. & Thompson, D. B., 1982. *Sedimentary Structures*. Allen and Unwin, London, 207 pp.

Drake, T. G., 1990. Structural features in granular flows. *Journal of Geophysical Research*, B95: 8681–8696.

Dumas, S. & Arnott, R. W. C., 2006. Origin of hummocky and swaley cross-stratification – The controlling influence of unidirectional current strength and aggradation rate. *Geology*, 34: 1073–1076.

Dziadzio, P., 2000. Depositional sequences in Badenian and Sarmatian deposits in the SE parts of the Carpathian Foredeep (SE Poland). *Przegląd Geologiczny*, 48: 1124–1138. [In Polish, English summary].

Dziadzio, P., Liszka, B., Maksym, A. & Stryszak, G., 1997. Środowisko sedymentacji utworów miocenu autochtonicznego w brzeżnej strefie Karpat, a interpretacja geologiczno-złożowa w obszarze Husów–Albigowa–Krasne. *Nafta-Gaz*, 53 (9): 407–414. [In Polish].

Dziadzio, P., Maksym, A. & Olszewska, B., 2006. Miocene deposits in the eastern part of the Carpathian Foredeep in Poland. *Przegląd Geologiczny*, 54: 413–420. [In Polish, English summary].

Dżułyński, S. & Walton, E. K., 1965. *Sedimentary Features of Flysch and Greywackes*. Elsevier, Amsterdam, 274 pp.

Eyles, N., Eyles, C. H. & Miall, A. D., 1983. Lithofacies types and vertical profile models; an alternative approach to the description and environmental interpretation of glacial diamict and diamictite sequences. *Sedimentology*, 30: 393–410.

Gingerich, P. D., 1969. Markov analysis of cyclic alluvial sediments. *Journal of Sedimentary Petrology*, 39: 330–332.

Harms, J. C., Southard, J. B., Spearing, D. R. & Walker, R. G., 1975. *Depositional Environments as Interpreted from Primary Sedimentary Structures and Stratification Sequences.* SEPM Short Course No. 2 Lecture Notes. Society of Economic Paleontologists and Mineralogists, Dallas, 161 pp.

Harper, C. W., Jr., 1984. Improved methods of facies sequence analysis. In: Walker, R. G. (ed.), *Facies Models*. 2nd Edition, Geoscience Canada Reprint Series 1, pp. 11–13.

Hiscott, R. N., 1994. Traction-carpet stratification in turbidites – Fact or fiction? *Journal of Sedimentary Research*, 64A: 204–208.

Jasionowski, M., 1997. Lithostratigraphy of the Miocene deposits in the eastern part of the Carpathian Foredeep. *Biuletyn Państwowego Instytutu Geologicznego*, 375: 43–60. [In Polish].

Karnkowski, P., 1999. *Oil and gas deposits in Poland*. The Geosynoptics Society GEOS. Kraków, pp. 379.

Kneller, B. C. & Branney, M. J., 1995. Sustained high-density turbidity currents and the deposition of thick massive sands. *Sedimentology*, 42: 607–616.

Komar, P. D., 1998. *Beach Processes and Sedimentation.* 2nd Edition, Prentice-Hall, Upper Saddle River, 544 pp.

Komar, P. D. & Miller, M. C., 1975. The initiation of oscillatory ripple marks and the development of plane-bed at high shear stresses under waves. *Journal of Sedimentary Petrology*, 45: 697–703.

Kotarba, M. J., Peryt, T. M. & Koltun, Y. V., 2011. Microbial gas system and prospectives of hydrocarbon exploration in Miocene strata of the Polish and Ukrainian Carpathian Foredeep. *Annales Societatis Geologorum Poloniae*, 81: 523–548.

Krumbein, W. C., Dacey, M. F., 1969. Markov chains and embedded Markov chains in geology. *Mathematical Geology*, 1: 69–79.

Krzywiec, P., 1999. Miocene tectonic evolution of the Eastern Carpathian Foredeep Basin (Przemyśl–Lubaczów) in light of seismic data interpretation. *Prace Państwowego Instytutu Geologicznego*, 168: 249–276. [In Polish, English summary].

Kurovets, I., Prytulka, G., Shpot, Y. & Peryt, T. M., 2004. Middle Miocene Dashava Formation sandstones, Carpathian Foredeep, Ukraine. *Journal of Petroleum Geology*, 27: 373–388.

Lewis, K. B., 1971. Slumping on a continental slope inclined as 1–4°. *Sedimentology*, 16: 97–100.

Lowe, D. R., 1982. Sediment gravity flows, II: Depositional models with special reference to the deposits of high-density turbidity currents. *Journal of Sedimentary Petrology*, 52: 279–297.

Lowe, D. R. 1988. Suspended-load fallout rate as an independent variable in the analysis of current structures. *Sedimentology*, 35: 765–776.

Lyzun, O., Kurovets, I., Prystulka, G., Sheremeta, O. & Zybko, O., 2004. Petrofizychni vlastyvosti porid-kolektoriv. In: Kolodiy, V. V., Boyko, G. Y., Boychevs'ka, L. E., Bratus', M. D & Velychko, N. S. (eds), *Karpats'ka naftogazonosna provintsiya*. Ukrains'kyy Vydavnychyy Tsentr, Lviv-Kyiv, pp. 130–146. [In Ukrainian].

Martinius, A. W., Ringrose, P. S., Brostrøm, C., Elfenbein, C., Næss, A. & Ringås, J. E., 2005. Reservoir challenges of heterolithic tidal sandstone reservoirs in the Halten Terrace, mid-Norway. *Petroleum Geoscience*, 11: 3–16.

Mastalerz, K., Wysocka, A., Krzywiec, P., Kasiński, J., Aleksandrowski, P., Papiernik, B. & Ryzer-Siupik, J., 2006. Miocene succession at the Ryszkowa Wola High (Sieniawa-Rudka area), Carpathian Foredeep Basin: facies and stratigraphic interpretation of wellbore and 3D seismic data. *Przegląd Geologiczny*, 54: 333–342. [In Polish, English summary].

Middleton, G. V. & Southard, J. B., 1978. *Mechanics of Sediment Movement*. Society of Economic Paleontologists and Mineralogists Short Course No. 3, March 29–30, Binghamton, New York, 159 pp.

Myrow, P. M. & Southard, J. B., 1991. Combined-flow model for vertical stratification sequences in shallow marine storm-deposited beds. *Journal of Sedimentary Petrology*, 61: 202–210.

Myrow, P. M. & Southard, J. B., 1996. Tempestite deposition. *Journal of Sedimentary Research*, 66: 875–887.

Myśliwiec, M. 2004. Traps for gas accumulations and the resulting zonation of the gas fields in the Miocene strata of the eastern part of the Carpathian Foredeep (SE Poland). *Przegląd Geologiczny*, 52: 657–664. [In Polish, English summary].

Myśliwiec, M., Madej, K. & Byś, I., 2004. The Miocene gas fields in the Rzeszów area, Carpathian Foredeep, on the base of the direct hydrocarbon Indicators. *Przegląd Geologiczny*, 52: 501–506. [In Polish, English summary].

Nemec, W., 1990. Aspects of sediment movement on steep delta slopes. In: Colella, A. & Prior, D. B. (eds), *Coarse-grained Deltas*. *International Association of Sedimentologists*, *Special Publication*, 10: 29–73.

Nemec, W., 1995. The dynamics of deltaic suspension plumes. In: Oti, M. N. & Postma, G. (eds), *Geology of Deltas*. Balkema, Rotterdam, pp. 31–93.

Ney, R., Burzewski, W., Bachleda, T., Górecki, W., Jakóbczak, K. & Słupczyński, K., 1974. Outline of paleogeography and evolution of lithology and facies of Miocene layers on the Carpathian Foredeep. *Prace Geologiczne*, 82: 1–65. [In Polish, English summary].

Nordahl, K., Ringrose, P. S. & Wen, R., 2005. Petrophysical characterization of a heterolithic tidal reservoir interval using a process-based modelling tool. *Petroleum Geoscience*, 11: 17–28.

Oszczypko, N., 1996. The Miocene dynamics of the Carpathian Foredeep in Poland. *Przegląd Geologiczny*, 44: 1007–1019. [In Polish, English summary].

Oszczypko, N., 2006. Development of the Polish sector of the Carpathian Foredeep. *Przegląd Geologiczny*, 54: 396–403. [In Polish, English summary].

Oszczypko, N., Krzywiec, P., Popadyuk, I. & Peryt, T., 2006. Carpathian Foredeep Basin (Poland and Ukraine): Its sedimentary, structural, and geodynamic evolution. In: Golonka, J. & Picha, F. J. (eds), *The Carpathians and Their Foreland: Geology and Hydrocarbon Resources*. *American Association of Petroleum Geologist Memoir*, 84: 393–350.

Parsons, J. D., Bush, J. W. M. & Syvitski, J. P. M., 2001. Hyperpycnal plume formation from riverine outflows with small sediment concentrations. *Sedimentology*, 48: 465–478.

Peryt, D., 1997. Calcareous nannoplankton stratigraphy of the Middle Miocene in the Gliwice area (Upper Silesia, Poland). *Bulletin of the Polish Academy of Sciences, Earth Sciences*, 45: 119–131.

Peryt, D., 1999. Calcareous nannoplankton assemblages of the Badenian evaporites in the Carpathian Foredeep. *Biuletyn Państwowego Instytutu Geologicznego*, 387: 158–161.

Peryt, T. M., 2006. The beginning, development and termination of the Middle Miocene Badenian salinity crisis in Central Paratethys. *Sedimentary Geology*, 188–189: 379–396.

Pietsch, K., Porębski, S. J. & Marzec, P., 2010. The use of seismostratigraphy for exploration of Miocene gas-gearing reservoirs in the NE part of the Carpathian Foreland Basin (Poland). *Geologia*, 36: 173–186. [In Polish, English summary].

Popadyuk, I., Vul, M., Landyzhensky, G. & Shapak, P., 2006. The petroleum geology of the Ukrainian Carpathian Foredeep. In: Golonka, J. & Picha, F. J. (eds), *The Carpathians and their foreland: Geology and hydrocarbon resources. American Association of Petroleum Geologist Memoir*, 84: 443–454.

Porębski, S. J., Meischner, D. & Gorlich, K., 1991. Quaternary mud turbidites from the South Shetland Trench (West Antarctica): recognition and implications for turbidite facies modelling. *Sedimentology*, 38: 691–715.

Porębski, S. J., Pietach, K., Hodiak, R. & Steel, R. J., 2002. Origin and sequential development of Upper Badenian – Sarmatian clinoforms in the Carpathian Foredeep Basin, SE Poland. *Geologica Carpathica*, 54: 119–136.

Porębski, S. J. & Steel, R. J., 2003. Shelf-margin deltas: their stratigraphic significance and relation to deep-water sands. *Earth-Science Reviews*, 62: 283–326.

Porębski, S. J. & Warchoł, M., 2006. Hyperpycnal flows and deltaic clinoforms – implications for sedimentological interpretation of late Middle Miocene fill in the Carpathian Foredeep Basin. *Przegląd Geologiczny*, 54: 421–429. [In Polish, English summary].

Reineck, H.-E. & Singh, I. B., 1975. *Depositional Sedimentary Environments.* 2nd Edition, Springer-Verlag, Berlin, 439 pp.

Ringrose, P., Nordahl, K. & Wen, R., 2005. Vertical permeability estimation in heterolithic tidal deltaic sandstones. *Petroleum Geoscience*, 11: 29–36.

Sztano, O. & De Boer, P. L., 1995. Basin dimensions and morphology as a controls on amplification of tidal motions (the Early Miocene North Hungarian Bay). *Sedimentology*, 42: 665–682.

Ślączka, A., Kruglov, S., Golonka, J., Oszczypko, N. & Popadyuk, I., 2006. Hydrocarbon Resources of the Outer Carpathians, Poland, Slovakia, and Ukraine: General Geology, In: Golonka, J. & Picha, F. J. (eds), *The Carpathians and their foreland: Geology and hydrocarbon resources. American Association of Petroleum Geologist Memoir*, 84: 443–454.

Vyalov, O. S., 1965. *Stratigrafiya neogenovykh molas Karpatskogo progiba*. Naukova Dumka, Kiev, 192 pp. [In Russian].

Warchoł, M., 2011. Przepływy hiperpiknalne i kryteria wyróżniania ich osadów w zapisie kopalnym. Unpublished PhD Thesis, Institute of Geological Sciences, Polish Academy of Sciences, Kraków, 296 pp. [In Polish].

Weber, K. J., 1982. Influence of common sedimentary structures on fluid flow in reservoir models. *Journal of Petroleum Technology*, 34: 665–672.

Weber, K. J., 1986. How heterogeneity affects oil recovery. In: Lake, L. W. & Carroll, H. B., Jr. (eds), *Reservoir Characterization*. Academic Press, Orlando, pp. 487–544.

Wysocka, A., 2002. Clastic Badenian deposits and sedimentary environments of the Roztocze Hills across the Polish-Ukrainian border. *Acta Geologica Polonica*, 52: 535–561.